

# Hydrodynamic stability of flow between rotating porous cylinders with radial and axial flow

Eric C. Johnson and Richard M. Lueptow

*Department of Mechanical Engineering, Northwestern University, Evanston, Illinois 60208*

(Received 10 September 1996; accepted 3 September 1997)

A linear stability analysis was carried out for axial flow between a rotating porous inner cylinder and a concentric, stationary, porous outer cylinder when radial flow is present for several radius ratios. The radial Reynolds number, based on the radial velocity at the inner cylinder and the inner radius, was varied from  $-15$  to  $15$ , and the axial Reynolds number based on the mean axial velocity and the annular gap was varied from  $0$  to  $10$ . Linear stability analysis for axisymmetric perturbations results in an eigenvalue problem that was solved using a numerical technique based on the Runge–Kutta method combined with a shooting procedure. At a given radius ratio, the critical Taylor number at which Taylor vortices first appear for radial outflow decreases slightly for small positive radial Reynolds numbers and then increases as the radial Reynolds number becomes more positive. For radial inflow, the critical Taylor number increases as the radial Reynolds number becomes more negative. For a given radial Reynolds number, increasing the axial Reynolds number increases the critical Taylor number for transition very slightly. The critical wave velocity decreases slightly for small positive radial Reynolds numbers, but increases for larger positive and all negative radial Reynolds numbers. The perturbed velocities are very similar to those for no axial flow. © 1997 American Institute of Physics. [S1070-6631(97)03812-9]

## I. INTRODUCTION

The linear stability of circular Couette flow in the annulus between a rotating inner cylinder and a concentric, fixed outer cylinder has been studied from both theoretical and experimental standpoints. The instability appears as pairs of counter-rotating, toroidal vortices stacked in the annulus. Taylor<sup>1</sup> conducted a simple flow visualization experiment to confirm his analytic prediction for the onset of the instability. Chandrasekhar,<sup>2</sup> DiPrima and Swinney,<sup>3</sup> Kataoka,<sup>4</sup> and Koschmeider<sup>5</sup> provide extensive summaries of the abundant research on this topic since Taylor's pioneering work.

The stability of Taylor vortex flow is altered when an additional flow is superimposed on the circular Couette flow. An axial flow in the annulus stabilizes the circular Couette flow so that the transition to supercritical Taylor vortex flow occurs at a higher Taylor number.<sup>6–13</sup> When the vortices appear, they translate in the same direction as the bulk axial flow in the annulus.<sup>12,14–16</sup> The axial flow can also alter the character of the flow instability, resulting in helical vortices and wavy helical vortices.<sup>15–19</sup> Recently, circular Couette flow with an axial flow has been used as a model for the study of the distinction between absolutely unstable flow, where a localized perturbation grows in both the upstream and downstream direction, and convectively unstable flow where a localized perturbation is advected downstream.<sup>13,20–22</sup> In this case, the type inflow boundary condition at the end of the finite length annulus can modify the vortex structure near the ends of the vortex system.<sup>22</sup>

A radial flow in the annulus between differentially rotating porous cylinders also affects the stability of the Taylor vortex flow. Radially inward flow and strong radially outward flow have a stabilizing effect. On the other hand, a weak radially outward flow destabilizes the flow.<sup>23–28</sup> Min and Lueptow<sup>27,28</sup> suggest an explanation that is based on the

incipient vortical motion related to supercritical flow first appearing near the inner cylinder.<sup>10,11</sup> A radially inward flow washes the incipient vortical motion out of the annulus through the porous inner cylinder. Likewise a strong radial outflow washes the incipient vortical motion across the annulus and out through the outer porous cylinder. Both situations stabilize the flow. However, weak radially outward flow carries the incipient supercritical motion into the annulus, resulting in transition at a lower Taylor number.

A combination of radial flow and axial flow superimposed on circular Couette flow occurs during dynamic filtration using a rotating filter.<sup>29–37</sup> In these devices an axial flow introduces a suspension into the annulus between a rotating porous inner cylinder and a stationary nonporous outer cylinder. Filtrate passes radially through the porous wall of the rotating inner cylinder, while the concentrate is retained in the annulus. The Taylor vortices appearing in the device are believed to wash the filter surface of the inner cylinder clean of particles, thus preventing the plugging of pores of the filter medium.<sup>38</sup> Centrifugal forces acting on the particles in suspension and the shear resulting from the rotation of the inner cylinder, are also thought to inhibit particles from plugging the pores of the filter.<sup>39</sup>

In this study we apply a linear hydrodynamic stability analysis to determine the critical Taylor number along with the associated wave number and wave velocity for the transition from stable circular Couette flow to vortical flow when there is a radial flow between two concentric, infinitely long, porous cylinders as well as an axial flow in the annulus. A sketch of the flow configuration is shown in Fig. 1. Little research has been done on the stability of circular Couette flow for the case of both radial flow (inflow or outflow) and axial flow. The narrow gap case for a similar problem involving corotating porous cylinders with an axial flow was studied by Bahl and Kapur,<sup>40</sup> but they made several problem-

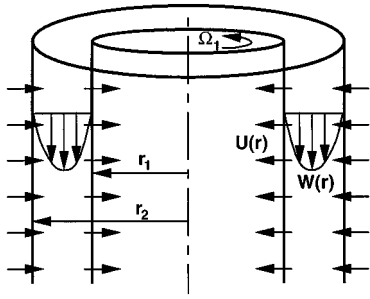


FIG. 1. Sketch of the flow configuration. The radial flow can be inward ( $\alpha < 0$ ) as shown or outward ( $\alpha > 0$ ).

atic simplifying assumptions in their analysis. They used the average axial velocity, which has been shown to cause errors.<sup>14,20</sup> In addition, they prescribed arbitrary values for the axial wave number and amplification factor based on analyses for no radial flow and the problematic average axial velocity. Unlike Bahl and Kapur we use the full linear disturbance equations and do not make the simplifying assumption of flow in a narrow gap, nor do we make any approximations regarding the axial velocity. Furthermore we directly calculate the axial wavenumber and amplification factor rather than specifying arbitrary values. Finally, we study the case where the outer cylinder is fixed, rather than rotating, because of the practical significance of this case. Quite recently, Kolyshkin and Vaillancourt<sup>41</sup> considered both axisymmetric and nonaxisymmetric convective instabilities for the inner cylinder and both cylinders rotating. They found that radially inward and strong radially outward flow stabilizes, whereas weak radially outward flow destabilizes the Couette flow, much like the situation when there is no axial flow. Their stability predictions match experiments reasonably well at low axial Reynolds numbers. Our work differs from Kolyshkin and Vaillancourt in that we consider a broader range of radial Reynolds numbers and address the dependence of the instability on the radius ratio. We also investigate the mode shapes of the velocity disturbances and the dependence of the wave velocity on the radial Reynolds number, neither of which were addressed previously.

The analysis that we use provides the stability boundary below which the flow is absolutely stable. We do not consider the convective instability. The flow configuration shown in Fig. 1 is obviously not identical to that in a rotating filter separator because the outer cylinder is porous. The flow in a rotating filter, however, is not easily amenable to analysis, although there has recently been work in that direction.<sup>42</sup> Nevertheless, analysis of the flow configuration in Fig. 1 can provide insight into the stability of flow in rotating filter separators because of the simultaneous existence of axial flow, radial flow, and circular Couette flow.

## II. ANALYTICAL FORMULATION

The Navier–Stokes and continuity equations in cylindrical coordinates  $(r, \theta, z)$  for steady, incompressible flow in the absence of a body force are used to find the stable solution

for axial and radial flow between an infinitely long rotating inner cylinder and a fixed concentric outer cylinder. The velocity field  $(U, V, W)$  is

$$U(r) = \frac{u_1 r_1}{r} = \frac{\alpha \nu}{r}, \quad (1a)$$

$$V(r) = Ar^{\alpha+1} + \frac{B}{r}, \quad (1b)$$

$$W_0(r) = \beta \frac{\nu}{d} C_0 \left[ \left( \frac{r}{d} \right)^2 + D_0 \ln \left( \frac{r}{d} \right) + E_0 \right], \quad \text{for } \alpha = 0, \quad (1c)$$

$$W_1(r) = \beta \frac{\nu}{d} C_1 \left[ \left( \frac{r}{d} \right)^2 + D_1 \left( \frac{r}{d} \right)^\alpha + E_1 \right], \quad \text{for } \alpha \neq 0. \quad (1d)$$

Here  $\alpha = u_1 r_1 / \nu$  is the radial Reynolds number and  $\beta = \bar{w} d / \nu$  is the axial Reynolds number, where  $u_1$  is the radial velocity through the wall of the inner porous cylinder with a positive value when outward from the axis of rotation,  $\bar{w}$  is the average axial velocity,  $d = r_2 - r_1$  is the gap between the cylinders, and  $\nu$  is the kinematic viscosity. The coefficients  $A, B, C_0, D_0, E_0, C_1, D_1,$  and  $E_1$  are functions of the radius ratio  $\eta = r_1 / r_2$  based on the boundary conditions at the walls and are given in Appendix A. It can be shown (using MATHEMATICA<sup>43</sup>) that  $W_1$  is equivalent to  $W_0$  in the limit as  $\alpha$  approaches zero. For no radial or axial flow,  $\alpha = \beta = 0$ , the equations revert to the solution for circular Couette flow between impermeable cylinders.<sup>2</sup> When there is no axial flow,  $\beta = 0$ , the equations are identical to those for circular Couette flow between porous cylinders.<sup>25,27</sup> And for no radial flow,  $\alpha = 0$ , the equations are the same, though in a slightly different form, as those used by Recktenwald *et al.*<sup>20</sup> for axial flow superimposed on circular Couette flow.

Low axial Reynolds numbers are associated with the axisymmetric supercritical instability for experiments of circular Couette flow with an axial flow<sup>13,15–19,44</sup> and circular Couette flow with an axial flow and a radial flow at the inner cylinder.<sup>28,41</sup> Since we consider relatively small axial Reynolds numbers, the stability problem is based on small axisymmetric perturbations  $u_r, u_\theta,$  and  $u_z$  of the velocity field and  $p'$  the pressure field. The perturbations are expressed as normal modes of the form

$$\begin{aligned} u_r &= e^{qt} u(r) e^{ikz}, \\ u_\theta &= e^{qt} v(r) e^{ikz}, \\ u_z &= e^{qt} w(r) e^{ikz}, \\ p' &= e^{qt} \omega(r) e^{ikz}, \end{aligned} \quad (2)$$

where  $k$  is the axial wave number of the disturbance,  $q$  is an amplification factor, and  $u(r), v(r), w(r),$  and  $\omega(r)$  are the amplitudes of the perturbations. The axial dependence of the perturbations in (2) is consistent with infinitely long cylinders. For circular Couette flow with an axial flow between finite length cylinders, Büchel *et al.*<sup>22</sup> have shown that the vortex structure near the ends of the annulus is strongly affected by the end boundary conditions, but the vortex structure in the bulk of the flow is unaffected. We expect a similar

effect when a radial flow is added, but ignore it since it does not significantly affect the vortex structure away from the ends of the annulus.

Substitution of (2) into the unsteady, incompressible, axisymmetric Navier–Stokes and continuity equations followed by linearization by discarding higher-order terms, results in the following equations for the amplitudes of the perturbed quantities

$$v \left( DD_* - k^2 - \frac{q}{\nu} - \frac{ikW}{\nu} \right) u + \frac{2V}{r} v - u DU - U Du = D\omega, \quad (3)$$

$$v \left( DD_* - k^2 - \frac{q}{\nu} - \frac{ikW}{\nu} \right) v - u D_* V - U D_* v = 0, \quad (4)$$

$$v \left( D_* D - k^2 - \frac{q}{\nu} - \frac{ikW}{\nu} \right) w - U Dw - u DW = ik\omega, \quad (5)$$

$$D_* u = -ikw, \quad (6)$$

where  $i$  is the square root of  $-1$ ,  $W$  is either  $W_0$  or  $W_1$  depending on the value of  $\alpha$ , and the following notation is established to simplify the equations:

$$D = \frac{d}{dr}, \quad D_* = \frac{d}{dr} + \frac{1}{r}. \quad (7)$$

Substituting the expression for  $w$  from (6) into (5) and then substituting the resulting expression for  $\omega$  into (3), results in

$$\begin{aligned} & \frac{\nu}{k^2} \left( D_* D - k^2 - \frac{q}{\nu} \right) (DD_* - k^2) u - \frac{1}{k^2} (DU) DD_* u \\ & - \frac{1}{k^2} UD^2(D_* u) + D(uU) - \frac{i}{k} \left( W(DD_* - k^2) u \right. \\ & \left. + \frac{u}{r} DW - uD^2W \right) = \frac{2V}{r} v. \end{aligned} \quad (8)$$

Rearrangement of (4) results in

$$v \left( DD_* - k^2 - \frac{q}{\nu} - \frac{ikW}{\nu} \right) v = u D_* V + U D_* v. \quad (9)$$

When there is no axial flow,  $W=0$ , these expressions are identical to those of Min and Lueptow<sup>27</sup> for circular Couette flow with radial flow only.

We now introduce the following dimensionless length scale  $r'$ , wave number  $a$ , amplification factor  $\sigma$ , and velocity perturbations  $u'$ ,  $v'$ , and  $w'$ :

$$r' = \frac{r}{d}, \quad a = kd, \quad \sigma = \frac{q}{\nu} d^2, \quad u' = \frac{u}{r_1 \Omega_1}, \quad (10)$$

$$v' = \frac{v}{r_1 \Omega_1}, \quad w' = \frac{w}{r_1 \Omega_1}.$$

At this point the derivation for the zero radial flow case corresponding to Eq. (1c) differs from that for the nonzero radial flow case corresponding to Eq. (1d). The more general nonzero radial flow case is derived here. The derivation for the zero radial flow case is very similar and the results are included in Appendix B. Substituting (1a), (1b), (1d), and (10) into (9), and solving for the radial velocity perturbation  $u(r)$  results in

$$u = u' r_1 \Omega_1 = \frac{\nu r_1 \Omega_1}{A(\alpha+2)d^{\alpha+2}} \left( \frac{\left( D' D_* - a^2 - \sigma - ia\beta C_1(r'^2 + D_1 r'^\alpha + E_1) - \frac{\alpha}{r'} D_* \right) v'}{r'^\alpha} \right). \quad (11)$$

From (6) and (11) axial velocity perturbation  $w(r)$  can be expressed as

$$w = w' r_1 \Omega_1 = \frac{i}{a} \frac{\nu r_1 \Omega_1}{A(\alpha+2)d^{\alpha+2}} D_* \left( \frac{\left( D' D_* - a^2 - \sigma - ia\beta C_1(r'^2 + D_1 r'^\alpha + E_1) - \frac{\alpha}{r'} D_* \right) v'}{r'^\alpha} \right). \quad (12)$$

Note that both  $u$  and  $w$  are expressed as functions of the azimuthal velocity perturbation  $v' = v/r_1 \Omega_1$ . All that is left is to find an expression for  $v'$ . Substituting (1a), (1b), (1d), and (10) into (8) results in

$$\begin{aligned} & (D' D_* - a^2 - \sigma)(D' D_* - a^2) u + \frac{\alpha}{r'^2} D' D_* u - \frac{\alpha}{r'} D'^2(D_* u) + \left( \frac{\alpha a^2}{r'} D' u - \frac{\alpha a^2}{r'^2} u \right) - ia\beta C_1[(r'^2 + D_1 r'^\alpha + E_1) \\ & \times (D' D_* - a^2) + (2\alpha - \alpha^2) D_1 r'^{\alpha-2}] u = 2 \frac{a^2 d^2}{\nu} \left( A r'^\alpha d^\alpha + \frac{B}{r'^2 d^2} \right) v' r_1 \Omega_1. \end{aligned} \quad (13)$$

Letting  $u_*$  represent the quantity in the outer parentheses in (11) and (12), dropping the prime notation, and rearranging the right-hand side of the equation yields

$$\begin{aligned} & (DD_* - a^2 - \sigma)(DD_* - a^2) u_* + \frac{\alpha}{r^2} DD_* u_* - \frac{\alpha}{r} D^2(D_* u_*) + \frac{\alpha a^2}{r} Du_* - \frac{\alpha a^2}{r^2} u_* - ia\beta C_1[(r^2 + D_1 r^\alpha + E_1)(DD_* - a^2) \\ & + (2\alpha - \alpha^2) D_1 r^{\alpha-2}] u_* = -Tr^\alpha \left( \frac{(1-\eta)^{\alpha+2}}{r^{\alpha+2}} - (1-\eta)^{2\alpha+4} \right) a^2 v, \end{aligned} \quad (14)$$

where

$$T = \frac{2(\alpha+2)\Omega_1^2}{v^2} \frac{r_1^2 r_2^2 \eta^2}{(1-\eta^{\alpha+2})^2} = \text{Ta}^2 \frac{2(\alpha+2)\eta^2}{(1-\eta^{\alpha+2})^2(1-\eta)^2}. \quad (15)$$

$T$  is a special form of the Taylor number that can be related to the Taylor number,  $\text{Ta} = \Omega_1 r_1 d / v$ . (We refer to the rotating Reynolds number,  $\text{Ta}$ , as the Taylor number to avoid confusion with the other two Reynolds numbers in the problem.) Note that (14) is an ordinary differential equation for the nondimensional azimuthal velocity perturbation  $v'(r)$ . For the case of no axial flow ( $\beta=0$ ), (14) reduces to an equation nearly identical to Eq. (14) of Min and Lueptow<sup>27</sup> for pure radial flow between a rotating porous inner cylinder and a stationary porous outer cylinder. The difference between the two equations arises from the different length scales used for nondimensionalization.

The perturbation velocity amplitudes  $u'$ ,  $v'$ , and  $w'$  must vanish on the boundaries at the inner cylinder,  $r'_1 = \eta/(1-\eta)$ , and the outer cylinder,  $r'_2 = 1/(1-\eta)$ . Using (11) and (12) and the boundary condition that  $v' = 0$  on the walls, the boundary conditions on the three perturbation velocity amplitudes,  $u'$ ,  $v'$ , and  $w'$ , can be written in terms of  $v'$  as

$$\frac{d^2 v}{dr^2} + \frac{(1-\alpha)}{r} \frac{dv}{dr} = 0, \quad (16a)$$

$$v = 0, \quad (16b)$$

$$\frac{d^3 v}{dr^3} - \left( \frac{(1-\alpha)^2 + 2}{r^2} + a^2 + \sigma + ia\beta C_1(r^2 + D_1 r^\alpha + E_1) \right) \frac{dv}{dr} = 0, \quad (16c)$$

where the prime notation has been dropped. This completes the derivation for the case when radial flow is present ( $\alpha \neq 0$ ). Equation (14) incorporating (15) along with the boundary conditions (16) provide equations that can be solved for the azimuthal velocity perturbation  $v$ . Equations (11) and (12) permit the calculation of the radial and axial velocity perturbations from  $v$ .

Equation (14) is a sixth-order ordinary differential equation for which the real part of the amplification factor  $\sigma$  is zero at the onset of the instability. Subjecting Eq. (14) to boundary conditions (16) leads to an eigenvalue problem, with the ultimate goal being the determination of the minimum Taylor number  $\text{Ta}$  and the associated wave number  $a$  and amplification factor  $\sigma$  that satisfy the ordinary differential equation and the boundary conditions for specified flow conditions  $\alpha$  and  $\beta$  at the specified geometry  $\eta$ .

To solve the problem a shooting method similar to the one used by Sparrow *et al.*<sup>45</sup> was used. First, a trial value of  $\text{Ta}$  was selected. Then three trial solutions,  $v_I$ ,  $v_{II}$ , and  $v_{III}$ , were constructed that satisfy Eq. (14) for prescribed values of  $\alpha$ ,  $\beta$ , and  $\eta$ , along with trial values for  $a$  and  $\sigma$ . All three trial solutions satisfied the boundary conditions at the inner wall (16) for  $v$ ,  $d^2 v / dr^2$ , and  $d^3 v / dr^3$ . But each trial solu-

tion satisfied a different set of boundary conditions for  $dv/dr$ ,  $d^4 v / dr^4$ , and  $d^5 v / dr^5$  at the inner wall, accomplished by, in each case, setting one of these three boundary conditions to unity and the remaining two to zero. A forward integration scheme (Runge–Kutta) was used to compute each trial solution using the six initial conditions at  $r'_1 = \eta/(1-\eta)$  for each of the trial solutions. In general, a linear combination of the trial solutions satisfies each of the boundary conditions (16) at  $r'_2 = 1/(1-\eta)$ . This can be written as

$$\begin{aligned} c_1 f_I + c_2 f_{II} + c_3 f_{III} &= 0, \\ c_1 g_I + c_2 g_{II} + c_3 g_{III} &= 0, \\ c_1 h_I + c_2 h_{II} + c_3 h_{III} &= 0, \end{aligned} \quad (17)$$

where  $f_i$ ,  $g_i$ , and  $h_i$  are the left-hand sides of boundary conditions (16a), (16b), and (16c), respectively, evaluated for the trial solution  $v_i$  at  $r'_2$ . The Runge–Kutta integration of Eq. (14) for the three trial solutions was repeated for several values of  $\text{Ta}$  until one was found, denoted  $\text{Ta}^*$ , that yielded a determinant of zero for the three by three matrix formed from  $f_i$ ,  $g_i$ , and  $h_i$ . Though this  $\text{Ta}^*$  indicates the onset of instability for the chosen values of  $a$  and  $\sigma$ , these are not necessarily the values that a system would achieve. In order to find the proper values, the above procedure was repeated varying both  $a$  and  $\sigma$ . For an arbitrarily chosen  $\sigma$ ,  $\text{Ta}^*$  may be complex. Since the imaginary part of  $\text{Ta}^*$  must be zero for physical situations,  $\sigma$  was varied until a real  $\text{Ta}^*$  was found. In practice, this was achieved by using real trial  $\text{Ta}^*$  and varying  $\sigma$  until the real and imaginary parts of the determinant vanished. Then the wave number  $a$  was varied and the process described above was repeated until the critical wave number for which  $\text{Ta}^*$  is a minimum was found. This minimum Taylor number is the critical Taylor number,  $\text{Ta}_c$ . Using the values of  $f_i$ ,  $g_i$ , and  $h_i$  evaluated for the critical Taylor number and the corresponding  $a$  and  $\sigma$  in Eq. (17) permits the calculation of the scaling factors  $c_2$  and  $c_3$  in terms of  $c_1$ . The perturbed velocity is the linear combination of the trial solutions,

$$v' = c_1 v_I + c_2 v_{III} + c_3 v_{III}. \quad (18)$$

Thus, the azimuthal velocity perturbation  $v'$  was calculated to within a multiplicative factor  $c_1$ .

Equation (14) was solved numerically using the Runge–Kutta solver built into MATHEMATICA.<sup>43</sup> This solver uses a variable step size, making adjustments to best approximate the actual solution. Because of the time required for the computations, typically only two decimal places of accuracy were used for the calculation of the critical wave number, and three decimal places of accuracy were possible for the calculation of the critical Taylor number and the critical wave speed, which is related to the amplification factor  $\sigma$ , as described shortly. A limitation of the MATHEMATICA solver is the difficulty in controlling the accuracy of the computations, which becomes evident in small errors in the wave number calculations, as discussed shortly.

TABLE I. Critical values for  $Ta$ ,  $a$ , and  $c$ .

(a) No radial flow ( $\alpha=0$ ) and no axial flow ( $\beta=0$ ).											
Radius ratio $\eta$	Roberts (Ref. 46)		Chung and Astill (Ref. 9)		Min and Lueptow (Ref. 27)		Recktenwald, <i>et al.</i> (Ref. 20)		Present		
	$a$	$Ta_c$	$a$	$Ta_c$	$a$	$Ta_c$	$a$	$Ta_c$	$a$	$Ta_c$	
0.95	3.13	184.98	3.13	184.99	3.13	184.99	...	...	3.13	184.99	
0.85	3.13	108.31	...	...	3.13	108.32	...	...	3.13	108.31	
0.75	3.14	85.78	3.14	85.78	3.14	85.78	3.1354	85.78	3.14	85.78	
0.65	3.14	74.96	...	...	...	...	...	...	3.14	74.96	

(b) Radial flow with no axial flow ( $\beta=0$ ).							
Radius ratio $\eta$	Radial Reynolds #		Min and Lueptow (Ref. 27)			Present	
	$\alpha$		$a$	$Ta_c$		$a$	$Ta_c$
0.95	15		...	176.48		3.13	176.48
	0		3.13	184.99		3.13	184.99
	-15		...	201.64		3.16	201.57
0.85	15		...	108.54		3.24	108.57
	0		3.13	108.32		3.13	108.31
	-15		...	155.76		3.34	155.79
0.75	15		...	107.74		3.49	107.76
	0		3.14	85.78		3.14	85.78
	-15		...	184.51		3.76	184.50

(c) Axial flow with no radial flow ( $\alpha=0$ ).																		
Radius ratio $\eta$	Axial Reynolds # $\beta$	Chung and Astill (Ref. 9)			DiPrima and Pridor (Ref. 14)			Ng and Turner (Ref. 12)			Babcock, <i>et al.</i> (Ref. 13)		Recktenwald, <i>et al.</i> (Ref. 20)			Present		
		$a$	$c$	$Ta_c$	$a$	$c$	$Ta_c$	$a$	$c$	$Ta_c$	$a$	$Ta_c$	$a$	$c$	$Ta_c$	$a$	$c$	$Ta_c$
0.95	0.01	...	...	...	3.13	1.170	184.99	3.127	1.170	184.99	...	...	...	...	3.13	1.170	184.99	
0.90	0.01	...	...	...	3.13	1.170	131.61	...	...	...	...	...	3.129	1.170	131.61	3.13	1.170	131.61
	10	...	...	...	3.14	1.169	136.63	...	...	...	...	...	3.139	1.169	136.63	3.08	1.168	136.64
0.75	2	3.148	1.172	85.99	...	...	...	...	...	...	3.136	85.91 <sup>a</sup>	3.136	1.172	85.91	3.13	1.17	85.91
	5	3.163	1.172	86.60	...	...	...	...	...	...	3.139	86.60 <sup>a</sup>	3.138	1.172	86.59	3.12	1.171	86.61
	10	3.165	1.172	89.02	...	...	...	...	...	...	3.145	89.02 <sup>a</sup>	3.146	1.171	89.02	3.08	1.169	89.07

<sup>a</sup>Values were calculated based on an expression for the reduced Taylor at  $\eta=0.74$  using  $Ta_c$  at  $\alpha=\beta=0$  from the present study.

The radial Reynolds number  $\alpha$  was varied from  $-15$  to  $15$  in increments of  $1$  near  $\alpha=0$  and increments of  $5$  for  $|\alpha|\geq 5$ , avoiding a singularity at  $\alpha=-2$ . The axial Reynolds number  $\beta$  was varied over the range for which axisymmetric disturbances are expected,<sup>9,15-17</sup> from  $0$  to  $10$ , in increments of  $1$  to  $5$ . The problem was solved for three radius ratios  $\eta$  of  $0.65$ ,  $0.75$ , and  $0.85$ . Calculations were also made for  $\eta=0.90$  and  $\eta=0.95$ , but because of the extremely long run times associated the large radius ratios and large axial Reynolds numbers, only a few calculations were made.

To assure the validity of our procedure we compared our results to previously published results for three cases: (1) no radial flow ( $\alpha=0$ ) and no axial flow ( $\beta=0$ );<sup>9,20,27,46</sup> (2) pure radial flow with no axial flow ( $\beta=0$ );<sup>27</sup> (3) no radial flow ( $\alpha=0$ ) with pure axial flow.<sup>9,12-14,20</sup> The similarity of the values for the critical Taylor numbers  $Ta_c$ , critical wave numbers  $a$ , and critical wave velocities  $c$  (to be defined shortly), shown in Table I, confirm that our procedure is valid. There is, however, a problem with the wave number calculations at high axial Reynolds numbers, as indicated in Table 1(c). Other calculations indicate that the wave number increases slightly with the axial Reynolds number. Our calculations indicate a very slight drop in the critical wave number as the axial Reynolds number increases from  $0$  to  $5$ . Then there is a somewhat larger decrease in the critical wave num-

ber as the axial Reynolds number increases from  $5$  to  $10$ . The reason for this contradiction is probably related to our computational accuracy. In the computations, it is necessary to determine the wave number for which the Taylor number is smallest. But relatively large changes in the wave number result in very small variations in the Taylor number. For instance, changing the wave number from the critical value of  $3.122$  to  $3.130$  (about  $0.26\%$ ) results in a change in the Taylor number from  $86.598\ 73$  to  $86.599\ 18$ , only  $0.0005\%$ , for a typical case of  $\alpha=0$ ,  $\beta=5$ , and  $\eta=0.75$ . This makes identifying the exact wave number corresponding to the minimum Taylor number quite difficult. Nevertheless, the critical Taylor number and wave speed are not strongly dependent on the wave number, so the results for these quantities match other calculations quite well.

### III. RESULTS AND DISCUSSION

The critical Taylor number for transition from stable circular Couette flow to supercritical Taylor vortex flow is shown in Fig. 2 as a function of the radial Reynolds number  $\alpha$  for two representative axial Reynolds numbers ( $\beta=0$  and  $\beta=10$ ). The curves for the other axial Reynolds numbers that were calculated ( $\beta=1,2,5$ ) lie between those plotted in Fig. 2 and are omitted for clarity. Radial inflow, correspond-

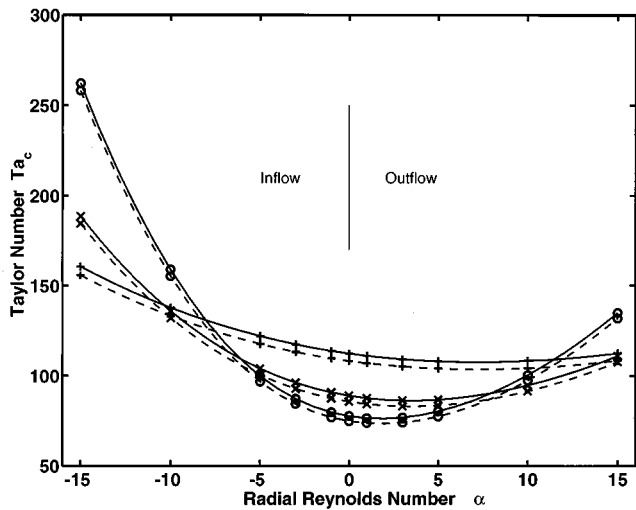


FIG. 2. The effect of the radial Reynolds number  $\alpha$  on the critical Taylor number  $Ta_c$ . Here  $\beta=0$  (no axial flow), dashed curves;  $\beta=10$ , solid curves;  $\eta=0.65$ ,  $\circ$ ;  $\eta=0.75$ ,  $\times$ ;  $\eta=0.85$ ,  $+$ . Curves are cubic spline fits to the data.

ing to negative radial Reynolds numbers, increases the critical Taylor number for the onset of instability, indicating a stabilizing effect. Similarly, strong radial outflow, corresponding to large positive radial Reynolds numbers, also stabilizes the flow. However, weak radial outflow, corresponding to small positive radial Reynolds numbers, destabilizes the flow by slightly decreasing the critical Taylor numbers. These results are consistent with those of Kolyshkin and Vaillancourt<sup>41</sup> and Bahl and Kapur<sup>40</sup> for nonzero  $\beta$ , although they considered much smaller ranges of  $\alpha$  at different radius ratios.

The effect of the radius ratio on the critical Taylor number is also evident in Fig. 2. For radial Reynolds numbers near zero, the transition to supercritical Taylor vortex flow occurs at a higher Taylor number as the annular gap narrows, or, in other words, as the radius ratio  $\eta$  increases. For larger negative or positive radial flows the opposite situation occurs. The transition to supercritical flow occurs at a higher Taylor number as the annular gap widens as a result of the stronger stabilizing effect of the radial flow for small radius ratios. In other words, the degree to which varying the radial Reynolds number affects the critical Taylor number lessens with narrowing gap. It is also evident that the upturn of the curve related to the stabilizing effect of strong radial outflow occurs at a smaller positive radial Reynolds number as the radius ratio decreases.

Min and Lueptow<sup>27,28</sup> offer a physical explanation for the effect of the radial flow on the stability based on the location of the first appearance of incipient vortical motion. Although stability theory indicates that the flow becomes universally unstable once the critical Taylor number is exceeded, the incipient vortical motion first appears near the rotating inner cylinder and then propagates radially outward as the Taylor number increases when no radial flow is present and the outer cylinder is stationary.<sup>10,11</sup> In the presence of radial inflow, the fluid where the incipient vortical motion begins is washed out of the annulus through the po-

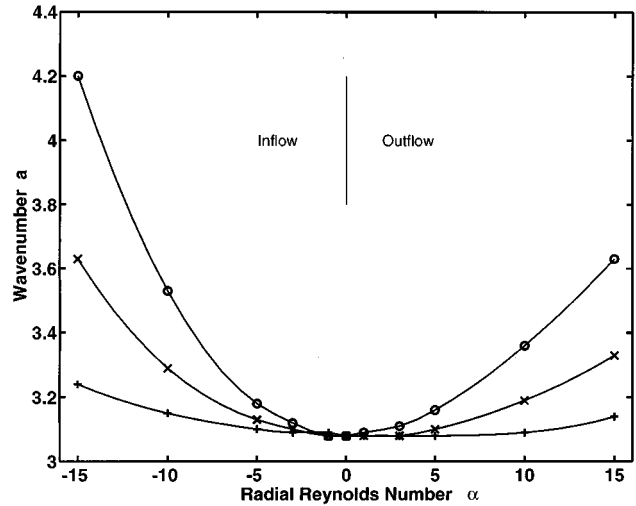


FIG. 3. The effect of the radial Reynolds number  $\alpha$  on the critical wave number  $a$  for  $\beta=10$ ;  $\eta=0.65$ ,  $\circ$ ;  $\eta=0.75$ ,  $\times$ ;  $\eta=0.85$ ,  $+$ . Curves are cubic spline fits to the data.

rous inner cylinder. Thus, the critical Taylor number for the onset of instability increases. Weak radial outflow, on the other hand, washes the incipient vortical motion away from the inner cylinder and outward across the annulus, resulting in a lower Taylor number for transition to supercritical flow. Strong radial outflow delays the onset of supercritical vortices by washing the incipient motion across the annulus and through the outer porous cylinder.

Increasing the axial Reynolds number increases the stability of the flow, although the effect is small over the range of axial Reynolds numbers considered. The curves for  $\beta=0$  and  $\beta=10$  are very close to one another, and the curves for the other axial Reynolds numbers ( $\beta=1, 2$ , and  $5$ ) are between these curves, but are omitted for clarity. The physical explanation for the stabilizing effect that an axial flow has on circular Couette flow is not clear. Perhaps the shear due to the axial flow somehow disrupts the incipient vortical motion near the inner cylinder, thus leading to the stabilizing effect.

The radial flow also affects the value of the critical wave number, shown in Fig. 3, keeping in mind that computational difficulties have resulted in slightly low values of the wave number. The critical wave number for the narrower gap is less affected by variations in the radial Reynolds number, while the effect in the wider gap is more pronounced. Both radial inflow and large radial outflow increase the critical wave number, although inflow has a greater effect than outflow for the same magnitude of the radial Reynolds number. Min and Lueptow<sup>27</sup> and Kolyshkin and Vaillancourt<sup>41</sup> found a similar result for the case of  $\beta=0$ , even noting a very slight decrease in wave number for small positive  $\alpha$ . Our data showed the same tendency as indicated by the less steeply sloped curves for radial outflow than for radial inflow, but we were unable to resolve the third decimal place of the wave number where this slight decrease would be evident because of unreasonably long computation times.

The supercritical vortices translate axially in the annulus when an axial flow is present. At the onset of the instability,

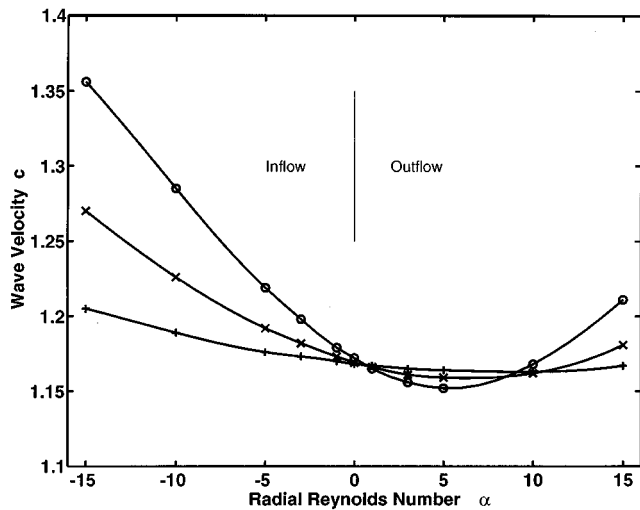


FIG. 4. The effect of radial Reynolds number  $\alpha$  on the critical wave velocity  $c$  for  $\beta=10$ ;  $\eta=0.65$ ,  $\circ$ ;  $\eta=0.75$ ,  $\times$ ;  $\eta=0.85$ ,  $+$ . Curves are cubic spline fits to the data.

the real part of the amplification factor  $q$  is zero, while the imaginary part of  $q$  is the dimensional frequency of the instability. As a result,  $iq$  divided by the dimensional axial wave number  $k$  of the instability represents the axial wave velocity of the instability. It is convenient to represent the critical wave speed as a fraction of the average axial velocity in the annulus  $\bar{w}$ , so that  $c = (iq/k)/\bar{w} = i\sigma/a\beta$ . The dependence of the critical wave velocity on the radial Reynolds number is shown in Fig. 4 for an axial Reynolds number of  $\beta=10$ . With the exception of the no-axial flow case where  $c=0$  (since the vortices are of a stationary cellular nature), the wave velocity is essentially insensitive to the axial Reynolds number over the range of consideration. As a result, the data for other axial Reynolds numbers ( $\beta=1,2,5$ ) overlay the data shown in Fig. 4. A very small decrease in the wave velocity was detected with increasing axial Reynolds number consistent with the results of Chung and Astill,<sup>9</sup> DiPrima and Pridor,<sup>14</sup> and Recktenwald *et al.*,<sup>20</sup> as indicated in Table 1(c).

Like the critical Taylor number and critical wave number, the critical wave velocity is more sensitive to the radial Reynolds number for a wider gap. The critical wave velocity also increases with radial inflow and strong radial outflow, and decreases slightly for weak radial outflow. This is best seen for the wider gaps, where the sensitivity to the radial flow is more pronounced. The critical wave velocity matches the results of previous researchers at  $\alpha=0$  as indicated in Table 1(c). It also corresponds with the experimental results of Snyder<sup>17</sup> and Lueptow *et al.*<sup>16</sup> that vortices travel at a velocity of 1.0–1.4 times the bulk axial velocity.

The effect of the radial flow on the relative amplitude of the perturbed velocities is shown in Fig. 5 for  $\beta=0$  and  $\beta=10$  at three radial Reynolds numbers for a radius ratio of  $\eta=0.85$ . The perturbed azimuthal velocity was found to within a multiplicative factor  $c_1$  using Eq. (18). Then the radial and axial velocity perturbations were calculated using Eqs. (11) and (12). Since the scaling of the amplitudes of the perturbed velocity components can only be determined to

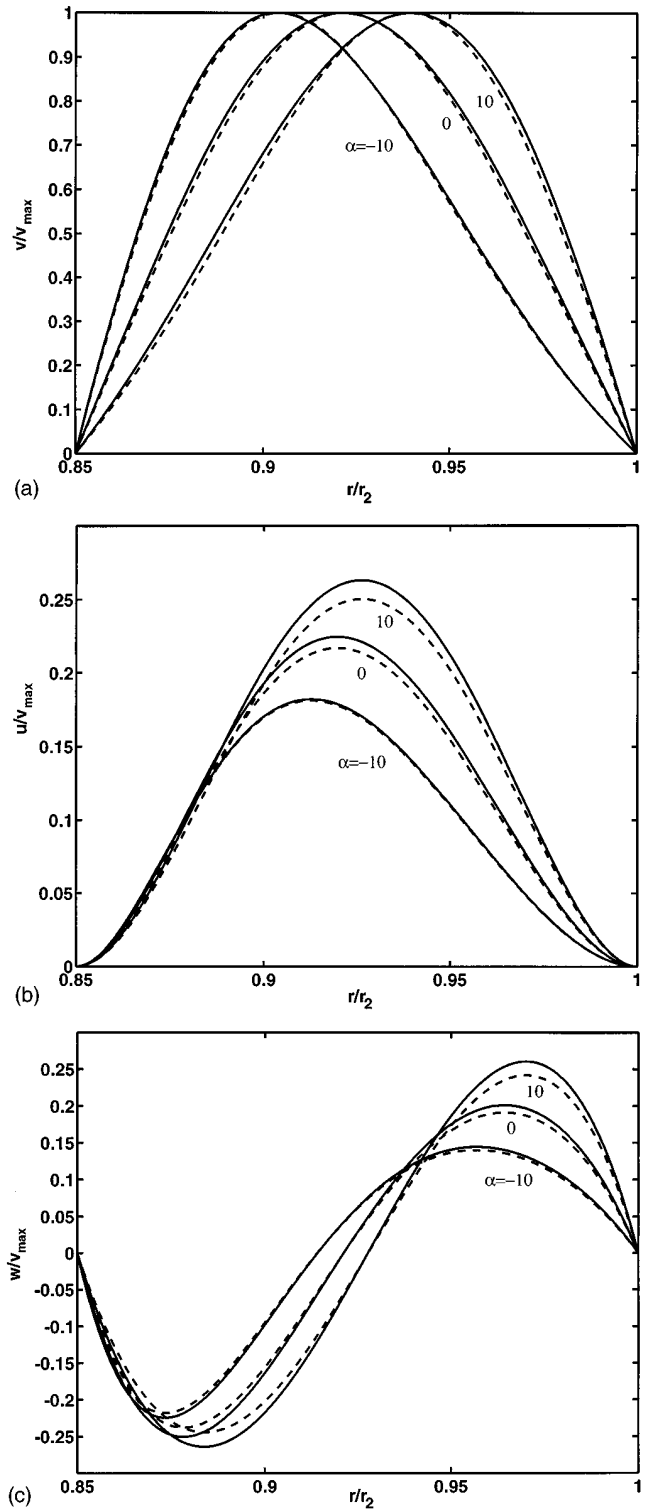


FIG. 5. The relative amplitude of the perturbation velocity from the inner cylinder at  $r/r_2=0.85$  to the outer cylinder at  $r/r_2=1$  for  $\eta=0.85$ . Here  $\beta=0$  (no axial flow), dashed curves;  $\beta=10$ , solid curves. (a) Relative amplitude of azimuthal perturbation velocity  $v/v_{\max}$ . (b) Relative amplitude of radial perturbation velocity  $u/v_{\max}$ . (c) Relative amplitude of axial perturbation velocity  $w/v_{\max}$ .

within a multiplicative factor, the amplitudes of the perturbed velocities are normalized by the maximum amplitude of the perturbed azimuthal velocity component,  $v_{\max}$ , for that particular Taylor number. In keeping with the proper

boundary conditions at the wall, the amplitudes of the perturbed velocities are zero at the inner wall,  $r_1/r_2 = \eta$ , and at the outer wall,  $r_2/r_2 = 1$ .

The effect of the radial flow on the perturbed velocities is the same as that found by Min and Lueptow:<sup>27</sup> the radial flow shifts the radial position of the maximum value of the relative amplitude of both the perturbed azimuthal velocity  $v$  and the perturbed radial velocity  $u$  in the direction of the radial flow, as shown in Figs. 5(a) and 5(b); radially inward flow suppresses the amplitude of the perturbed radial velocity  $u$  and the perturbed axial velocity  $w$ , while radial outflow amplifies these velocities, as shown in Figs. 5(b) and 5(c); and the zero crossing, minimum, and maximum of the perturbed axial velocity are shifted in the direction of the radial flow, as shown in Fig. 5(c).

Our key interest here is the effect of the axial flow on the perturbed velocities. The axial flow has very little effect on the perturbed azimuthal velocity, as is evident from the similarity between the dashed curves for  $\beta=0$  and the solid curves for  $\beta=10$  in Fig. 5(a). On the other hand, the axial flow results in a small increase in the amplitude of the radial and axial velocity perturbations for zero and positive radial flow ( $\alpha=0,10$ ), as shown in Figs. 5(b) and 5(c). But it has very little effect on the radial and axial velocity perturbations for a radial inflow ( $\alpha=-10$ ). Based on the results in Fig. 5, it is clear that the radial inflow has a substantial effect on the structure of the vortex flow, shifting the vortices radially inward or outward, depending on the direction of the radial flow. By comparison, the axial flow has only a minor effect on the relative amplitudes of the velocity perturbations.

#### IV. SUMMARY

The results of this analysis of flow between differentially rotating porous cylinders with an axial and radial flow indicate that radially inward flow stabilizes the flow, whereas *weak* radially outward flow slightly destabilizes the flow. This result is true, regardless of radius ratio and strength of the axial flow, although the effect is greater when the radius ratio is decreased. Although a weak radial outflow destabilizes the flow, a strong outflow stabilizes the flow. The critical wave number and critical wave velocity increase with radially inward flow and strong radially outward flow, although weak radially outward flow results in a small decrease in these quantities.

Axial flow always stabilizes the flow slightly for the range of axial Reynolds numbers considered, independent of the radial flow and radius ratio. Over the range of radial and axial flows considered, there is very little influence by the radial flow on the how much the axial flow increases the stability. The wave velocities have almost no dependence on the axial Reynolds number over the range considered.

The original motivation for this work was the flow in a rotating filter device. In such a device, only the inner cylinder is porous, while the outer cylinder is nonporous. The axial flow in the annulus provides the source of the fluid that flows radially inward through the inner porous cylinder. The case of a rotating filter is not easily amenable to analysis because no analytic stable solution exists for the flow and because the flow through the porous inner cylinder varies

with axial position. However, the results presented here provide several insights with regard to the rotating filter application. Typically in such devices,  $-10 < \alpha < -0.1$  at the inner cylinder and  $1 < \beta < 50$ .<sup>31,33-35,47,48</sup> The results presented here suggest that a slightly higher rotational speed is needed to assure the appearance of Taylor vortices in the annulus than if there were no radial flow. An axial flow also stabilizes the flow requiring a higher rotational speed for supercritical vortices to appear, although the effect of the axial flow is quite small.

#### ACKNOWLEDGMENTS

Support by Northwestern University and in part by the National Science Foundation are gratefully acknowledged.

#### APPENDIX A: VELOCITY FIELD COEFFICIENTS

The constants in Eq. (1) were found by applying the no-slip boundary condition at the walls of the inner and outer cylinder and by using the definition for the average axial velocity  $\bar{w}$ ,

$$A = \frac{-\Omega_1 \eta^2}{r_2^\alpha (1 - \eta^{\alpha+2})}, \quad (\text{A1})$$

$$B = \frac{r_1^2 \Omega_1}{1 - \eta^{\alpha+2}}, \quad (\text{A2})$$

$$C_0 = \frac{-2}{\left[ 1 + \frac{1}{1-\eta} \left( \frac{2\eta}{1-\eta} + \frac{1+\eta}{\ln \eta} \right) \right]}, \quad (\text{A3})$$

$$D_0 = \frac{1+\eta}{1-\eta} \frac{1}{\ln \eta}, \quad (\text{A4})$$

$$E_0 = \frac{1+\eta}{1-\eta} \frac{\ln(1-\eta)}{\ln \eta} - \frac{1}{(1-\eta)^2}, \quad (\text{A5})$$

$$C_1 = \frac{2(2+\alpha)(\eta^\alpha - 1)(1-\eta)^2}{(2-\alpha)(1-\eta^{\alpha+2}) + (2+\alpha)(\eta^2 - \eta^\alpha)}, \quad (\text{A6})$$

$$D_1 = \frac{(1-\eta^2)(1-\eta)^{\alpha-2}}{\eta^\alpha - 1}, \quad (\text{A7})$$

$$E_1 = \frac{\eta^2 - \eta^\alpha}{(\eta^\alpha - 1)(1-\eta)^2}. \quad (\text{A8})$$

#### APPENDIX B: EQUATIONS FOR ZERO RADIAL FLOW

The derivation for the case of no radial flow ( $\alpha=0$ ) is very similar to that where radial flow is nonzero, except for the expression for the stable axial flow,  $W$ . Thus, substituting (1a), (1b), (10), and (1c) rather than (1d) into (9), and solving for the radial velocity perturbation  $u(r)$ , results in

$$u = u' r_1 \Omega_1 = \frac{\nu r_1 \Omega_1}{2A d^2} [D' D'_* - a^2 - \sigma - ia\beta C_0(r'^2 + D_0 \ln r' + E_0)] v'. \quad (\text{B1})$$

From (6) and (B1), axial velocity perturbation  $w(r)$  is

$$w = w' r_1 \Omega_1 = \frac{i \nu r_1 \Omega_1}{a 2A d^2} D'_* \{ [D' D'_* - a^2 - \sigma - ia\beta C_0(r'^2 + D_0 \ln r' + E_0)] v' \}. \quad (\text{B2})$$

Letting  $u_*$  represent the quantity in the outermost brackets in (B1) and (B2), substituting (1a), (1b), (1c), and (10) into (8), and dropping the prime notation yields, after manipulation,

$$\begin{aligned} & (DD_* - a^2 - \sigma)(DD_* - a^2)u_* - ia\beta C_0 \\ & \times \left( (r^2 + D_0 \ln r + E_0)(DD_* - a^2) + \frac{2D_0}{r^2} \right) u_* \\ & = -T \left( \frac{(1-\eta)^2}{r^2} - (1-\eta)^4 \right) a^2 v. \end{aligned} \quad (\text{B3})$$

Equation (B3) for  $\alpha=0$  corresponds to Eq. (14) for  $\alpha \neq 0$ .

- <sup>1</sup>G. I. Taylor, "Stability of a viscous liquid contained between two rotating cylinders," *Philos. Trans. A* **223**, 289 (1923).  
<sup>2</sup>S. Chandrasekhar, *Hydrodynamic and Hydromagnetic Stability* (Oxford University Press, 1961).  
<sup>3</sup>R. C. DiPrima and H. L. Swinney, "Instabilities and transition in flow between concentric rotating cylinders," in *Topics in Applied Physics, Hydrodynamic Instabilities and the Transition to Turbulence*, edited by H. L. Swinney and J. P. Gollub (Springer-Verlag, Berlin, 1985), pp. 139–180.  
<sup>4</sup>K. Kataoka, "Taylor vortices and instabilities in circular Couette flows," in *Encyclopedia of Fluid Mechanics*, edited by N. P. Chermisnoff (Gulf Publishing Company, Houston, 1986), Vol. 1, pp. 237–273.  
<sup>5</sup>E. L. Koschmieder, *Benard Cells and Taylor Vortices* (Cambridge University Press, Cambridge, 1993).  
<sup>6</sup>J. Kaye and E. C. Elgar, "Modes of adiabatic and diabatic fluid flow in an annulus with an inner rotating cylinder," *Trans. ASME* **80**, 753 (1958).  
<sup>7</sup>S. Chandrasekhar, "The hydrodynamic stability of viscoid flow between coaxial cylinders," *Proc. Natl. Acad. Sci. USA* **46**, 141 (1960).  
<sup>8</sup>R. C. DiPrima, "The stability of a viscous fluid between rotating cylinders with an axial flow," *J. Fluid Mech.* **9**, 621 (1960).  
<sup>9</sup>K. C. Chung and K. N. Astill, "Hydrodynamic instability of viscous flow between rotating coaxial cylinders with fully developed axial flow," *J. Fluid Mech.* **81**, 641 (1977).  
<sup>10</sup>M. A. Hasoon and B. W. Martin, "The stability of viscous axial flow in an annulus with a rotating inner cylinder," *Proc. R. Soc. London, Ser. A* **352**, 351 (1977).  
<sup>11</sup>N. Gravas and B. W. Martin, "Instability of viscous axial flow in annuli having a rotating inner cylinder," *J. Fluid Mech.* **86**, 385 (1978).  
<sup>12</sup>B. S. Ng and E. R. Turner, "On the linear stability of spiral flow between rotating cylinders," *Proc. R. Soc. London, Ser. A* **382**, 83 (1982).  
<sup>13</sup>K. L. Babcock, G. Ahlers, and D. S. Cannell, "Noise-sustained structure in Taylor–Couette flow with through flow," *Phys. Rev. Lett.* **67**, 3388 (1991).  
<sup>14</sup>R. C. DiPrima and A. Pridor, "The stability of viscous flow between rotating concentric cylinders with an axial flow," *Proc. R. Soc. London, Ser. A* **366**, 555 (1979).  
<sup>15</sup>D. I. Takeuchi and D. F. Jankowski, "A numerical and experimental investigation of the stability of spiral Poiseuille flow," *J. Fluid Mech.* **102**, 101 (1981).  
<sup>16</sup>R. M. Lueptow, A. Docter, and K. Min, "Stability of axial flow in an annulus with a rotating inner cylinder," *Phys. Fluids A* **4**, 2446 (1992).  
<sup>17</sup>H. A. Snyder, "Experiments on the stability of spiral flow at low axial

- Reynolds numbers," *Proc. R. Soc. London, Ser. A* **265**, 198 (1962).  
<sup>18</sup>K. Bühler, "Instabilitäten spiralförmiger strömungen im zylinderspalt," *Z. Angew. Math. Mech.* **64**, T180 (1984).  
<sup>19</sup>K. Bühler and N. Polifke, "Dynamical behavior of Taylor vortices with superimposed axial flow," in *Nonlinear Evolution of Spatio-Temporal Structures in Dissipative Continuous Systems*, Vol. Series B: Physics edited by F. H. Busse and L. Kramer (Plenum Press, New York, 1990), Vol. 225, pp. 21–29.  
<sup>20</sup>A. Recktenwald, M. Lücke, and H. W. Müller, "Taylor vortex formation in axial through-flow: Linear and weakly nonlinear analysis," *Phys. Rev. E* **48**, 4444 (1993).  
<sup>21</sup>A. Tsameret, G. Goldner, and V. Steinberg, "Experimental evaluation of the intrinsic noise in the Couette–Taylor system with an axial flow," *Phys. Rev. E* **49**, 1309 (1994).  
<sup>22</sup>P. Büchel, M. Lücke, D. Roth, and R. Schmitz, "Pattern selection in the absolutely unstable regime as a nonlinear eigenvalue problem: Taylor vortices in axial flow," *Phys. Rev. A* **53**, 4764 (1996).  
<sup>23</sup>T. S. Chang and W. K. Sartory, "Hydromagnetic stability of dissipative flow between rotating permeable cylinders," *J. Fluid Mech.* **27**, 65 (1967).  
<sup>24</sup>T. S. Chang and W. K. Sartory, "Hydromagnetic stability of dissipative flow between rotating permeable cylinders. Part 2. Oscillatory critical modes and asymptotic results," *J. Fluid Mech.* **36**, 193 (1969).  
<sup>25</sup>S. K. Bahl, "Stability of viscous flow between two concentric rotating porous cylinders," *Def. Sci. J.* **20**, 89 (1970).  
<sup>26</sup>K. Bühler, "Taylor vortex flow with superimposed radial mass flux," in *Ordered and Turbulent Patterns in Taylor–Couette Flow*, edited by E. D. Andereck and F. Hayot (Plenum Press, New York, 1992), pp. 197–203.  
<sup>27</sup>K. Min and R. M. Lueptow, "Hydrodynamic stability of viscous flow between rotating porous cylinders with radial flow," *Phys. Fluids* **6**, 144 (1994).  
<sup>28</sup>K. Min and R. M. Lueptow, "Circular Couette flow with pressure-driven axial flow and a porous inner cylinder," *Exp. Fluids* **17**, 190 (1994).  
<sup>29</sup>K. H. Kroner, V. Nissinen, and H. Ziegler, "Improved dynamic filtration of microbial suspensions," *Bio/Technology* **5**, 921 (1987).  
<sup>30</sup>K. H. Kroner and V. Nissinen, "Dynamic filtration of microbial suspensions using an axially rotating filter," *J. Membrane Sci.* **36**, 85 (1988).  
<sup>31</sup>G. Beaudoin and M. Y. Jaffrin, "Plasma filtration in Couette flow membrane devices," *Artif. Organs* **13**, 43 (1989).  
<sup>32</sup>S. Wronski, E. Molga, and L. Rudniak, "Dynamic filtration in biotechnology," *Bioproc. Eng.* **4**, 99 (1989).  
<sup>33</sup>U. B. Holeschovsky and C. L. Cooney, "Quantitative description of ultrafiltration in a rotating filtration device," *AIChE J.* **37**, 1219 (1991).  
<sup>34</sup>G. Belfort, J. M. Pimbley, A. Greiner, and K. Y. Chung, "Diagnosis of membrane fouling using a rotating annular filter. 1. Cell culture media," *J. Membrane Sci.* **77**, 1 (1993).  
<sup>35</sup>G. Belfort, P. Mikulasek, J. M. Pimbley, and K. Y. Chung, "Diagnosis of membrane fouling using a rotating annular filter. 2. Dilute particle suspensions of known particle size," *J. Membrane Sci.* **77**, 23 (1993).  
<sup>36</sup>H. B. Winzeler and G. Belfort, "Enhanced performance for pressure-driven membrane processes: The argument for fluid instabilities," *J. Membrane Sci.* **80**, 35 (1993).  
<sup>37</sup>R. M. Lueptow and A. Hajiloo, "Flow in a rotating membrane plasma separator," *ASAIO J.* **41**, 182 (1995).  
<sup>38</sup>J. R. Hildebrandt and J. B. Saxton, "The use of Taylor vortices in protein processing to enhance membrane filtration performance," in *Bioprocess Engineering Colloquium*, edited by R. C. Dean Jr. and R. M. Nerem (The American Society of Mechanical Engineers, New York, 1987), pp. 93–95.  
<sup>39</sup>R. M. Lueptow, "Fluid mechanics of a rotating filter separator," *Advances in Filtration and Separation Technology*, Nashville, TN, American Filtration and Separations Society, 1995, pp. 283–291.  
<sup>40</sup>S. K. Bahl and K. M. Kapur, "The stability of a viscous flow between two concentric rotating porous cylinders with an axial flow," *Def. Sci. J.* **25**, 139 (1975).  
<sup>41</sup>A. Kolyshkin and R. Vaillancourt, "Convective instability boundary of Couette flow between rotating porous cylinders with axial and radial flow," *Phys. Fluids* **9**, 910 (1997).  
<sup>42</sup>F. Marques, J. Sanchez, and P. D. Weidman, "Generalized Couette–Poiseuille flow with boundary mass transfer," submitted to *J. Fluid Mech.*  
<sup>43</sup>S. Wolfram, *Mathematica: A System for Doing Mathematics by Computer* (Addison–Wesley, Redwood City, CA, 1991).  
<sup>44</sup>A. Tsameret and V. Steinberg, "Noise-modulated propagating pattern in a convectively unstable system," *Phys. Rev. Lett.* **67**, 3392 (1991).  
<sup>45</sup>E. M. Sparrow, W. D. Munro, and V. K. Jonsson, "Instability of the flow

- between rotating cylinders: The wide-gap problem," J. Fluid Mech. **20**, 35 (1964).
- <sup>46</sup>P. H. Roberts, "Appendix: The solution of the characteristic value problems," Proc. R. Soc. London, Ser. A **283**, 550 (1965).
- <sup>47</sup>W. Tobler, "Dynamic filtration: Principle and application of shear filtration in an annular gap," Filtr. Sep. **19**, 329 (1982).
- <sup>48</sup>K. Ohashi, K. Tashiro, F. Kushiya, T. Matsumoto, S. Yoshida, M. Endo, T. Horio, K. Ozawa, and K. Sakai, "Rotation-induced Taylor vortex enhances filtrate flux in plasma separation," Trans. Am. Soc. Artif. Intern. Organs **34**, 300 (1988).